

SHRINKAGE AND SWELLING PROPERTIES OF FLOCCULATED MATURE FINE TAILINGS

Yutian Yao¹, A. Frits van Tol^{1,2}, Leon van Paassen¹, Philip J. Vardon¹

¹Delft University of Technology, Delft, the Netherlands

²Deltares, Delft, the Netherlands

ABSTRACT

In the atmospheric fines drying technique, mature fine tailings (MFT) are treated with polymers and deposited in thin layers on a sloped surface for sub-aerial drying. During the whole drying period, the tailings deposits can experience rewetting during periods of rainy weather or as result of the the placement of new layers. This paper addresses the shrinkage and swelling behavior of flocculated MFT (FMFT) under drying and rewetting cycles. The shrinkage and swelling paths of tailing samples were assessed by laboratory experiments. The results showed that the shrinkage-swelling process in a FMFT sample is reversible once the initial drying did not extend below the shrinkage limit of the soil or the soil reached an equilibrium stage which occurred after at least four shrink-swell cycles. The effects of the flocculation procedure on the shrinkage behavior were investigated.

INTRODUCTION

In Alberta, the atmospheric fines drying technique is currently being implemented on a commercial scale. In general, this technique involves the deposition of polymer treated mature fine tailings (MFT) of the oil sands mining process in a thin layer on a sloped surface. Upon deposition, the released water flows to the lower point and it is collected and recycled to the oil extraction process. The remaining clay sediments are subjected to atmospheric conditions for natural drying. Once a layer of mud is dried, another layer is placed on top of it and this process is repeated to build a soil deposit. Desiccation is the dominant process in the whole disposal period, meanwhile, the flocculated MFT experience rewetting due to environmental factors (i.e. precipitation) and the placement of new layers. As a result, the tailing deposits undergo cyclic shrinkage and swelling. In geotechnical engineering, the shrinkage and swelling behavior of soils is usually presented by the soil shrinkage or swelling characteristics curve,

SSCC, in which the volumetric water content is plotted versus void ratio. The shrinkage curve for a soil is one of the soil property functions, which is required when undertaking numerical modeling studies to predict the mechanical behavior of unsaturated soils (Fredlund 2000). The shrinkage behavior of clays with high water content has been extensively studied in recent years. Fredlund et al. (2011) assessed the SSCC of MFT sludge and used it to determine the primary reference point of the soil water retention curve (SWRC). The rewetting properties of MFT or flocculated MFT, however, are seldom reported.

This paper summarizes some results of the experimental program conducted at Delft University of Technology on oil sands fine tailings. In this research, the shrinkage and swelling paths of FMFT during several drying and rewetting cycles were determined. The data obtained from these experiments provide an insight into the properties of flocculated MFT and are necessary input for numerical modelling (e.g. Vardon et al., 2014).

SHRINKAGE AND SWELLING THEORY

The soil shrinkage is defined as the specific volume change of soil relative to its water content. It can be measured in most soils with more than 10% clay content (Boivin et al., 2006). The shrinkage property of a soil is characterized by its shrinkage curve which is a normally presented as a water content-void ratio plot. Figure 1 shows a typical shrinkage curve for a saturated soil. Several different stages of deformation can be identified from the curve. These stages are: (a) structural shrinkage, (b) normal shrinkage, (c) residual shrinkage and (d) zero shrinkage (Haines, 1923; Stirk, 1954). The structural shrinkage occurs only in well-structured soils. In the case of clay paste, this stage doesn't exist. In the normal shrinkage, decrease in total volume is equal to the volume of water lost. At the end of this stage, air enters the voids at a point that is regarded as the general air entry point and it is quite close to the plastic limit of

the soil. In the next stage, decrease in water upon drying exceeds the volume change of the bulk soil. Finally, the bulk volume of the soil remains constant as the water volume further decreases. During this stage, reorganization of clay particles does occur, leading to the formation of microscopic cracks. (Bruand and Prost, 1987, Cornelis et al., 2006). The shrinkage limit of a soil is defined as the water content corresponding to the minimum volume that a soil can attain upon drying to zero water content. It can be used to evaluate the shrinkage potential, crack development potential, and swell potential of cohesive soils. The shrinkage limit is determined experimentally, it can also be inferred from the SSCC which is shown in the graph.

Proposed by Fredlund et al. (2002), the shrinkage curve of an unsaturated specimen is similar to the one shown in Figure 2. There are also three stages during drying. In the first shrinkage stage, the shrinkage curve follows the line for the constant degree of saturation that the soil possessed before shrinkage. In the last stage, the void ratio remains constant as the water content further decreases.

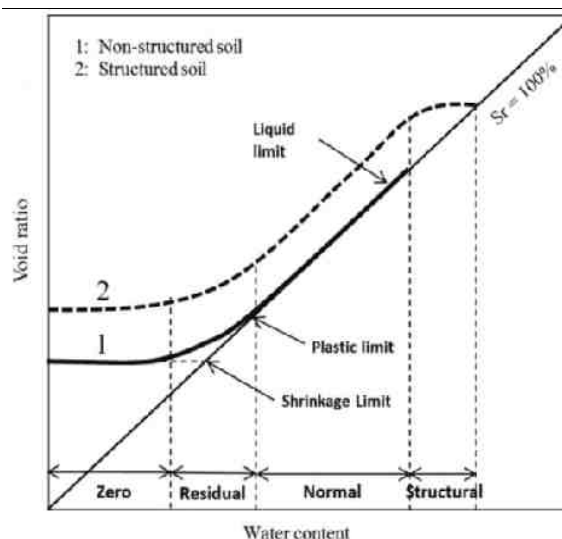


Figure 1. Typical SSCC for a nonstructured soil (solid line, 1) and a well-structured soil (dashed line, 2) after Cornelis et al. (2006)

Similar to the multistage shrinkage behavior of a soil, swelling of a desiccated soil also occurs in different stages that are, namely, (1) primary swelling, (2) secondary swelling and (3) zero swelling (Day, 1999). Most of the swelling completes in the primary swelling stage that occurs at a very rapid rate. In the second stage, some

microcracks close and the entrapped air further reduces. In the third phase, the soil reaches its maximum capacity of retaining water and no further volume changes take place.

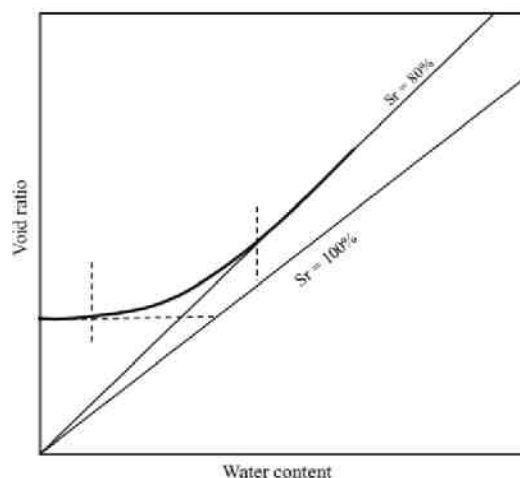


Figure 2. Schematic presentation of SSCC for a partially saturated clay after Fredlund et al. (2002)

MATERIALS AND METHODS

Materials and sampling method

MFT used in this program were obtained from Muskeg River Mine in Alberta, Canada. The MFT slurry contains 35% solids by weight and has a bulk density of 1200 kg/m³. Particle size analysis showed that approximately 90 % of solids are fines (<44 microns) and 60% of the material is classified as clay size particles (<2 microns). The specific gravity of the solids in MFT is 2.30. MFT sludge was flocculated by a high molecule weight polymer which was obtained from polymer company. Prior to flocculation, the MFT sludge was diluted to 21% in solids content suspension and about 500ml suspension was poured into a cylindrical mixing container which is 88 mm in diameter. A certain amount of polymer solution was injected into the tailings, then the MFT-polymer mixtures were agitated by a rotating paddle impeller which is 60 mm in diameter. The primary flocculation tests showed that the optimal dosage of polymer was 1000g dry polymers per ton of solids (1000g/t) and the optimal flocculation result was achieved when the mixtures were mixed at the speed of 200 rpm for 3 minutes. The optimum of flocculation result is defined as the fastest settling speed of flocs and the maximum amount of water released during 24

hours. After the mixing was completed, the sludge was allowed to settle for 24h and the released water was decanted. Next, the slurry was compressed in slurry consolidometer under air pressure (5-10 kPa) and oedometer (10-20 kPa) to remove excess water.

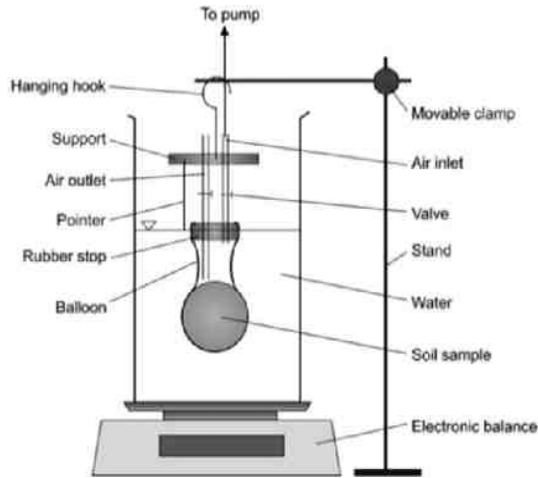


Figure 3. Setup for Tariq and Durnford balloon shrinkage test (Cornelis et al., 2006)

Soil shrinkage test

Determination of shrinkage curve requires continuous measurement of weight and bulk volume of a soil specimen during shrinkage. Two basic methods were employed to determine the SSCC. The first method (the geometry method) is to directly measure the dimension of the specimen at different stages of drying. The sample was confined in an oedometer ring and placed on a wax paper, and then the drying was commenced. At regular time intervals, the mass and dimension of soil were measured. The second method is called balloon shrinkage test developed by Tariq and Durnford (1993). The setup used in this test is shown in Figure 3. A soil clod (20-30 cm³) was inserted into a rubber balloon which was closed by a stopper with an air inlet and outlet. To allow drying, both valves were kept open and the air inlet was connected to an air pump which passed air at a low pressure (200 L/h) over the specimen. The mass of the specimen was measured by an electronic balance. The volume was determined by closing the air outlet and apply a small vacuum through the inlet to ensure a perfect fitting of the balloon around the soil sample, submerging the balloon under water and measuring the mass of

water replaced by the soil sample using the Archimedes principle. At the end of shrinkage, the soil sample was dried at 105 °C in the oven to calculate the water content at each measurement. The void ratio, e , and the degree of saturation, S_r , are calculated using the following formulas:

$$e = \frac{G_s(1+w)}{\rho_b} - 1 \quad (1)$$

$$S_r = \frac{G_s w}{e} \quad (2)$$

where G_s = specific gravity of solids, w = gravimetric water content, ρ_b = bulk density of soil.

Soil swelling test

Three different methods were used to investigate the swelling behavior. The first method is the volumetric swelling test performed with the oedometer device. The desiccated specimen was immersed under water in an oedometer cell and a surcharge pressure was applied on top of the specimen. The pressure applied was selected not to cause compression of the specimen during wetting process. The axial swelling of the specimen was monitored by a dial gauge that was connected to a computer. In the test two different boundary conditions were applied on the specimens. In the first condition, the only pressure applied on the specimen was the weight of the top loading cap. In this case, the soil was allowed to swell freely in both lateral and axial direction. In the second condition, the specimen was trimmed to be contained in an oedometer ring. During wetting, only axial swelling was allowed and measured.

In the second method, the tailing sample was wetted by applying a vacuum pressure (about 1 bar) in the vacuum saturation device. As shown in Figure 4, the soil specimen was contained in a steel ring between two pieces of porous stones and immersed under water in a vessel which is connected to the vacuum pump. During the saturation process, the lateral swelling is fully constrained while the axial swelling is partially constrained due to the elasticity of the rubber elastic. At different time, the total height (H) was measured using a caliper. Then the porous stones were removed and the weight of the soil and the ring) were determined. The third method is opposite to the shrinkage process, which aims to determine the rewetting paths of the SSCC. At the end of the shrinkage test, the soil sample (soil clod or cylindrical specimen) was immersed in water for

free swelling or confined swelling. The weight and volume of the sample were measured at different time by following the similar procedure to the shrinkage test. Prior to each measurement, free water left on the soil surface was removed by filter paper. To prevent collapse of the soil sample due to prolonged soaking, the cylindrical specimen was wound around by a plastic electrical tape (Figure 5). Since the electrical tape has some flexibility, the soil is in partially constrained condition in lateral direction.

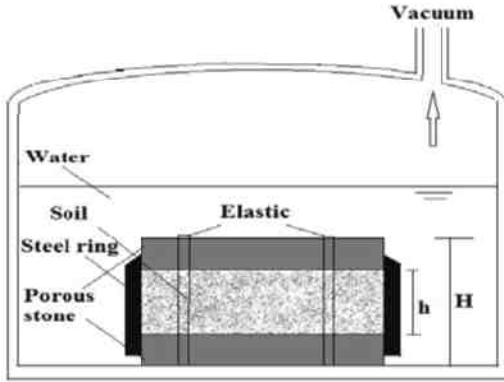


Figure 4. Vacuum saturation device used for rewetting of soil specimen



Figure 5. FMFT sample in the confinement of the electrical tape

RESULTS AND DISCUSSION

Shrinkage curve and shrinkage limit

Figure 6 provides the water content versus void ratio plots for saturated FMFT which were determined using the balloon method and the geometry method. The results obtained by the two methods were quite similar for the same material. However, the balloon method was capable of

generating a fluent curve which can be best fitted using the equation proposed by Fredlund et al. (1997, 2002, 2013). The equation has parameters with physical meaning, and is of the following form:

$$e(w) = a_{sh} \left(\frac{w^c}{b_{sh}^c} + 1 \right)^{\left(\frac{1}{c}\right)} \quad (3)$$

where a_{sh} = the minimum void ratio, b_{sh} = slope of the line of tangency, c = curvature of the shrinkage, w = gravimetric water content, and $a_{sh}/b_{sh} = G_s/S_r$ = constant for a specific soil. In this case, the fitted parameters are: $a_{sh} = 0.705$, $b_{sh} = 0.303$, $c = 6.693$ and $a_{sh}/b_{sh} = G_s/S_r = 2.33$. Note that the experimental data did not coincide perfectly with 100% saturation line in the normal shrinkage stage, which is probably due to the accuracy of measurement. According to the SSCC determined, the plastic limit of FMFT was close to 40% (0.4) and the shrinkage limit was 31% (0.31). The minimum void ratio attained by the specimen was 0.70.

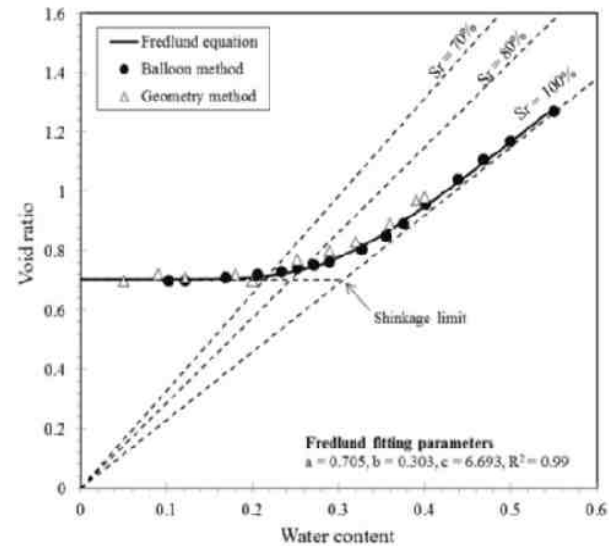


Figure 6. Observed SSCC for the flocculated MFT specimen (flocculated at the dosage of 1000g/t and mixed at 200 rpm for 2 min)

Swelling potential and swelling curves

Oedometer swelling tests provided information on the rate and magnitude of axial swelling for the tailings samples in different conditions. Figure 7 shows a time — vertical swell curve monitored for a desiccated FMFT (4% in water content) during free swelling. The three swelling stages (i.e.

primary, secondary and zero swelling) were identified from the curve. About 88% of total swelling completed in the first day upon wetting. The swelling speed then reduced significantly in the second stage and no swelling occurred in the third stage. Figure 8 shows the specimen at the end of swelling test, from which one can see a main horizontal crack and several minor vertical cracks on the side wall of the specimen. Occurrence of cracks could be attributed to the properties of FMFT and the method of experiment. In this case, microcracks may occur in the drying process due to reorganization of clay particles. Since there is no confinement on the soil during wetting, some of the cracks open up and grow bigger with increasing water content. The experimental results showed that this phenomenon was common for the FMFT samples when the specimen was not sufficiently confined during the long-term immersion in water. In this test, the total vertical swelling was 13% of the original height. The final void ratio and the saturation degree of the specimen were calculated using Eq. (2) and (3) and they were 1.17 and 90%, respectively. Note that in void ratio calculation the measured bulk volume of the soil contained the extra volume of cracks and it was larger than the real clay volume, thus the void ratio of the specimen was to some extent overestimated while the degree of saturation was underestimated.

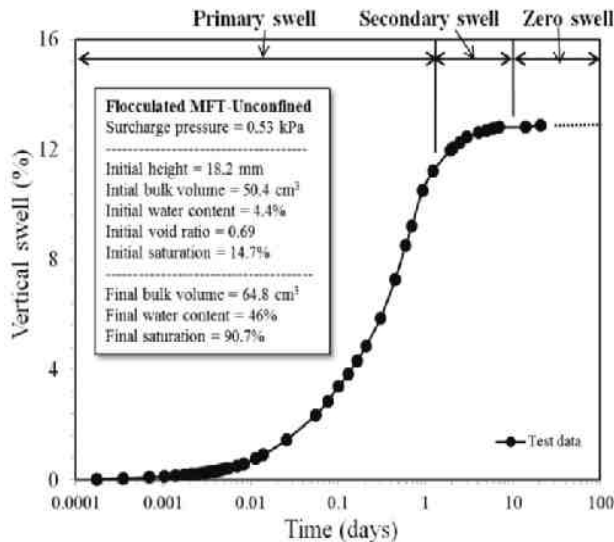


Figure 7. Vertical swell vs time curve determined for flocculated MFT in free swelling condition



Figure 8. FMFT specimen at the end of free swelling test

Table 1. Results of one-dimensional swelling tests for FMFT specimens

Sample ID	1	2	3	4
Surcharge (kPa)	1	1	1	20
Before swelling				
Height (mm)	16.6	19	19	15.2
Water content (%)	20	6	20	1.7
Void ratio	0.69	0.65	0.0.69	0.72
Saturation (%)	57	21	58	5.3
After swelling				
Height (mm)	20.6	22.9	23.0	15.8
Water content (%)	44	40	40	27
Void ratio	1.18	0.91	1.03	0.82
Saturation (%)	87	92	90	76
Swell potential	29	16	13	6

Table 1 offers the results of confined swelling tests. In this test, the FMFT samples were 50 mm in diameter and immersed in water under different surcharge pressures. The swell potential given in the table is calculated as:

$$\text{Swell potential} = \frac{\Delta e}{1+e_0} \times 100 \quad (4)$$

where Δe = increase in void ratio at the end of swelling, e_0 = void ratio of unsoaked sample. The results showed that the swelling potential of a specimen is related to its bulk volume, initial water content and surcharge pressure. In general, when the soil specimens are wetted in the same manner, the sample which initially has a smaller size, lower water content and lower surcharge pressure will have a larger swelling potential. Due to the lateral confinement of the ring, vertical cracks were not observed on the specimens, unlike for the free-swelling test (Figure 9). However, several very fine horizontal cracks occurred on the specimen,

except for Sample 4 which was under a significantly higher surcharge pressure. The final degree of saturation at the end of swelling was about 90% for samples 1, 2 and 3 and 73% for sample 4. As the free and confined swelling tests showed that the samples (provided they have an initial water content below 20%) did not reach full saturation upon rewetting under atmospheric conditions and apparently some entrapped air could not escape, the question was raised whether the desiccated tailings could reach a higher saturation value if they were saturated under vacuum conditions.

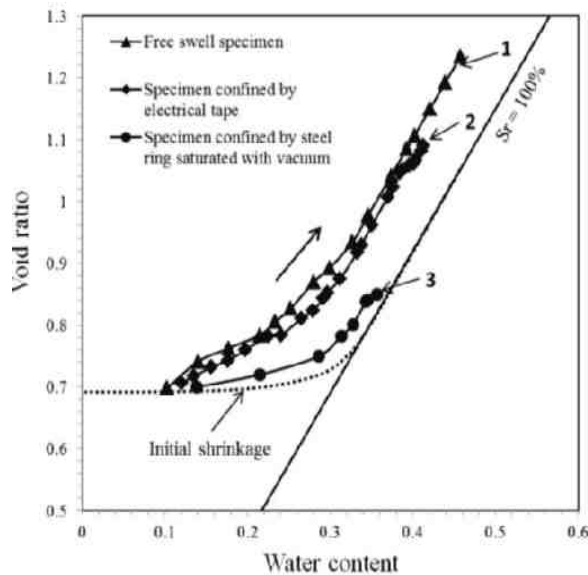


Figure 9. Rewetting curves for FMFT wetted in different conditions

Figure 9 shows the rewetting curves measured for different desiccated FMFT specimens. Specimen 1 and 2 were soaked with water in a container at atmospheric conditions. Specimen 1 was free swelling in all directions while specimen 2 was partially confined in lateral direction by an electrical tape (Figure 5). Specimen 3 was confined in a steel ring and saturated in a container under vacuum (Figure 4). It was seen that void ratios attained in the swelling path were higher than the corresponding values in the shrinkage path at the same water content, which is referred to as hysteresis. All of the swelling curves shared a similarity that two stages of swelling were identified. The first stage is a curvilinear portion with a higher tangent slope than the shrinkage curve in the same range of water content. In the second stage, the void ratio increases with the water content in a linear manner. The linear portion is parallel to the

100% saturation line. The results showed that the curve 1 and curve 2 were “parallel” to each other during the first and the early part of the second stage. At a water content of about 38%, the curve 2 bend off towards the 100% saturation line and formed a new line parallel to the 100% saturation line. Some fine cracks (0.1-0.2 mm) occurred on the specimen 1 and 2 during the second swelling phase. Reflected on the graph, the linear portion of the swelling path extended further since increase in bulk volume is equal to increase in crack volume. The curve 3 indicated that with the help of vacuum pressure (1 bar), most of the trapped air was discharged and thus a higher degree of saturation was obtained. Swelling cracks were successfully prevented due to the confinement of the steel ring and the porous stones. At the end of the second stage, the swelling curve approached the line of full saturation.

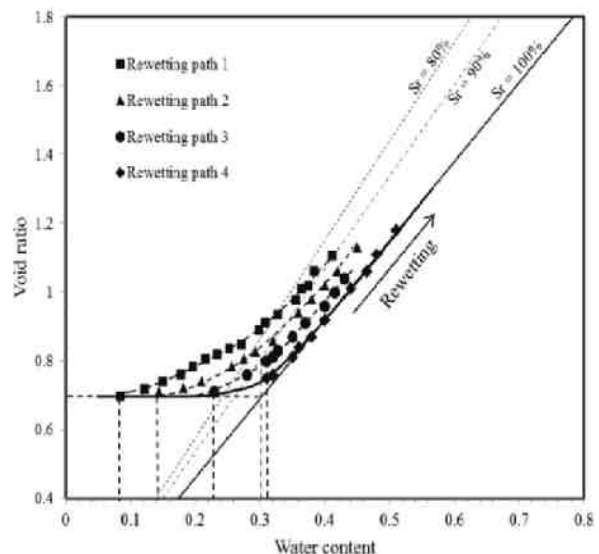


Figure 10. Effects of initial water content on the rewetting behaviors of FMFT

To evaluate the effect of the water content after drying on the swelling behavior of FMFT a couple of samples were dried to different water content. The specimens were then immersed under water without any confinement and the determined rewetting paths are shown in Figure 10. The graph shows that the rewetting paths are similar to each other in shape which consists of a curvilinear portion and a linear portion. As their initial water content decreases, length of the curvilinear portion increases and the residual saturation after rewetting. Note that for sample 4 which had the water content before swelling slightly higher than the shrinkage limit, the linear portion of the

swelling path coincided with the drying curve. We can conclude that once the soil drying does not extend below the shrinkage limit, the rewetting process is reversible. Otherwise, hysteresis occurs in the rewetting curves resulting a higher void ratio than the drying path.

Multiple shrinkage and swelling cycles

Figure 11 shows the shrink-swell paths of FMFT in the second drying and rewetting cycle. The soil specimen had the saturation degree of 86% at the end of the first shrinkage-swelling cycle. In the second cycle, the shrinkage path first followed the 86% saturation line before joining the initial shrinkage curve and ended at the same water content as the first drying process. The swelling path in the second cycle was above the drying path and it was almost the same as the swelling curve in the first cycle. Hysteresis in further drying and wetting paths reduced compared with the first cycle.

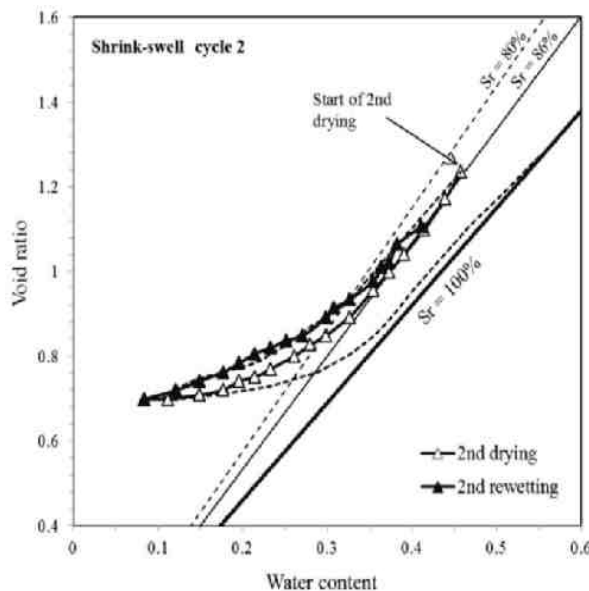


Figure 11. Shrinkage and swelling paths in the second drying and rewetting cycle

Based on the experimental results, a schematic presentation of the drying and rewetting paths is given in Figure 12. In this graph, point A is the minimum water content attained by the soil specimen during first drying process. When the soil specimen is rewetted at this point, the difference in void ratio between the rewetting and drying path

(hysteresis) is maximized. The linear portion of the rewetting path AD is parallel to the 100% saturation line. Once the soil is dried for the second time at the point D, the drying path will follow the saturation line 1 and finally arrive at point B which has the same void ratio as point A. It indicates that the shrinkage curve for a partially saturated specimen will finally reach the initial shrinkage curve for the fully saturated specimen. The second rewetting path BE and the third drying path EC is similar to the curve AD and DB, respectively. The slope of the linear portion of the rewetting path is always less than that of the drying path.

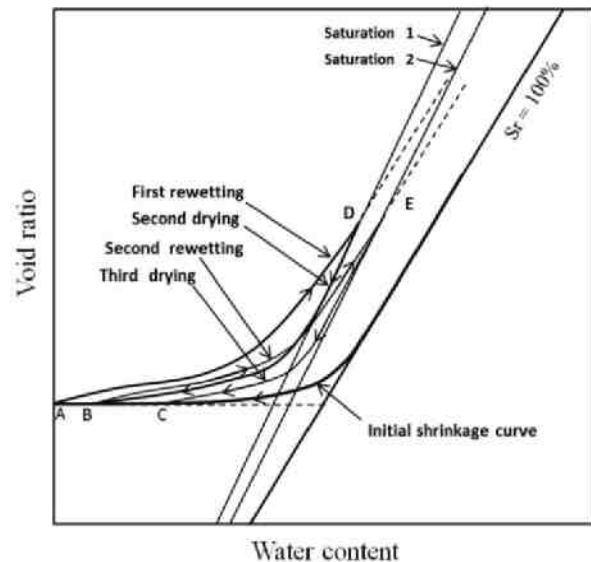


Figure 12. Schematic presentation of shrinkage and swelling curves for FMFT sample

Shrinkage and swelling behavior of a single desiccated FMFT specimen during five successive drying and rewetting cycles is illustrated in Figure 13. It was seen that hysteresis in drying and rewetting paths reduced with the increasing number of swell-shrink cycles. An equilibrium stage of soil occurred in the fourth cycle and the swell-shrink path was reversible. This phenomenon is quite similar to that observed by Tripathy et al. (2002) who performed drying and wetting tests on compacted expansive clay in four full swell-shrink cycles.

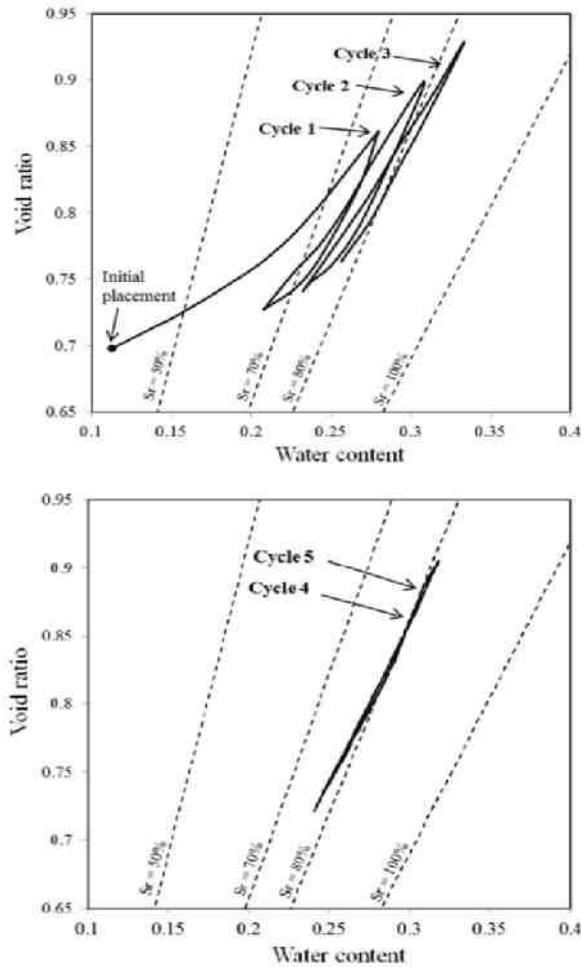


Figure 13. Shrinkage and swelling paths of the FMFT specimen in drying and wetting cycles

Effects of flocculation procedure

As indicated by Yao et al. (2012), the behavior of FMFT was affected by aspects of the flocculation procedure including type and dosage of polymer and mixing conditions. Figure 14 illustrates the effect of polymer dosage on the shrinkage characteristics of flocculated tailings. The curves showed that the minimum void ratio for the non-flocculated MFT was about 0.40 which increased to 0.57 and 0.7 after being treated with polymer at the dosage of 500g/t (0.5g/kg) and 1000g/t, respectively. The results indicate that, after being treated with polymer, the volume of the desiccated tailings increased by 12% and 25% for the FMFT specimens with 500g/t and 1000g/t, respectively.

Figure 15 shows the shrinkage results determined for FMFT samples that were mixed in different

conditions at a fixed dosage (1000g/t). In the residual and zero shrinkage stage, void ratios of the specimen varied with its mixing intensity and duration which is actually related to the mixing energy input. It indicates that when the specimen is over-mixed the final void ratio reduces relative to the specimen in optimal mixing condition. It is assumed that if the mixing is too intensive flocs are broken down and consequently leave an less open structure after settling and drying.

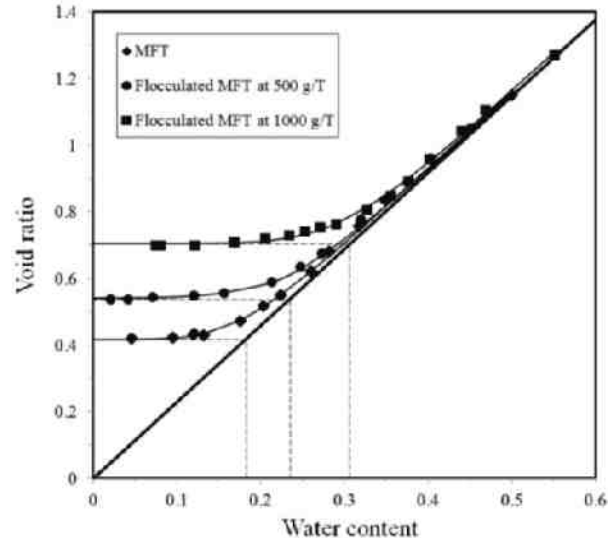


Figure 14. The shrinkage curves of tailings changing with polymer dosages

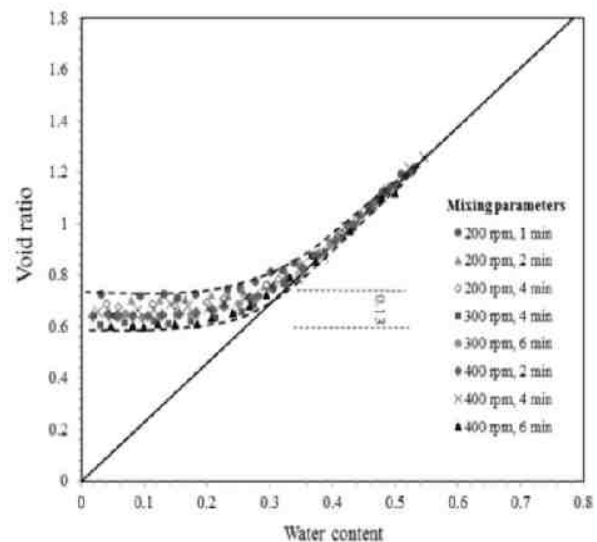


Figure 15. Effects of mixing conditions on the shrinkage curves of FMFT at 1000g/t

CONCLUSIONS

This paper explored the shrinkage/swelling behavior of flocculated MFT during drying and rewetting. The determined soil shrinkage characteristic curve (SSSC) showed that the shrinkage limit was 30% and the minimal void ratio was 0.7 for the tailing material that was treated by polymer at the dosage of 1000g/t and mixed at 200 rpm for 2 min.

Results of soil swelling tests showed that the rewetting properties of tailings were dependent on the initial water content, the confining pressure and the wetting method. Specimens with initial water contents below the shrinkage limit did not reach full saturation when allowed to soak up water under atmospheric conditions. When vacuum was used to rewet the soils full saturation was reached. In the free swelling condition, horizontal and vertical cracks occurred on the specimen which finally destructed the specimen. Therefore, the measured rewetting path of the specimen did not approach the fully saturation line. The determined rewetting curve consisted of a curvilinear portion and a linear portion that is parallel to the 100% saturation line.

Under the following conditions the shrink-swell process of the specimen is reversible: (1) when the initial drying process does not extend below the shrinkage limit of the soil and (2) when the soil is subjected to at least four shrink-swell cycles to reach an equilibrium stage. Otherwise, hysteresis occurs in the drying and rewetting paths showing larger void ratio in the wetting path than in the drying path.

Aspects of flocculation such as polymer dosage and mixing conditions can influence the properties of FMFT. Different polymer dosage results in different minimal void ratios of the specimen at the end of shrinkage, indicating a different volume of desiccated tailings.

REFERENCES

- Bruand, A., Prost, R., 1987. Effect of water content on the fabric of a soil material: an experimental approach. *Journal of Soil Science*, **38**: 461–472.
- Boivin, P., Garnier, P., and Vauclin, M., 2006. Modeling the soil shrinkage and water retention curves with the same equations. *Soil Science Society of America Journal*, **70**: 1082–1093.
- Cornelis, W. M., Corluy, J., Medina, H., Diaz, J., Hartmann, R., Van Meirvenne, M., & Ruiz, M. E. 2006. Measuring and modelling the soil shrinkage characteristic curve. *Geoderma*, 137(1), 179-191.
- Fredlund, M.D. 2000. Unsaturated soil property functions. Ph.D. dissertation. University of Saskatchewan, Saskatoon, 292 pp.
- Fredlund, M., Wilson, G. and Fredlund, D. 2002. Representation and estimation of the shrinkage curve. Third international conference on unsaturated soils. UNSAT, 2002. March 10-13, 2002, Recife, Brazil. 145-149.
- Fredlund D.G., Stone, J. and Stianson, J. 2011. Determination of water storage and permeability functions for oil sands tailings. *Proceedings tailings and mine waste 2011*. Vancouver, BC, Canada
- Haines, W. B., 1923. The volume changes associated with variations of water content in soil. *Journal of Agricultural Science*, **13**: 296–311.
- Stirk, G. B., 1954. Some aspects of soil shrinkage and the effect of cracking upon air entry into the soil. *Australian Journal of Soil Research*, **5**: 279–290.
- Tripathy S, Rao K S S, Fredlund D G. 2002. Water content-void ratio swell-shrink paths of compacted expansive soils[J]. *Canadian Geotechnical Journal*, 2002, 39(4): 938-959.
- Vardon, P. J., Nijssen, T., Yao, Y., van Tol, F. 2014. Numerical simulation of fine oil sand tailings drying in test cells. *Fourth International Oil Sands Tailing Conference (IOSTC'14)*.
- Yao. Y., van Tol, F. Van Paassen, L. 2012. The effect of flocculant on the geotechnical properties of mature fine tailings: an experimental study. *Proceedings of 3rd international oil sands tailings conference*. Edmonton, Alberta, Canada, December 2-5, 2012.